JACS
JOURNAL OF THE AMERICAN CHEMICAL SOCIETY

Article

Record Complexity in the Polycatenation of Three Porous Hydrogen-bonded Organic Frameworks with Stepwise Adsorption Behaviors

Yu-Lin Li, Eugeny V. Alexandrov, Qi Yin, Lan Li, Zhi-Bin Fang, Wenbing Yuan, Davide M. Proserpio, and Tian-Fu Liu

J. Am. Chem. Soc., **Just Accepted Manuscript** • DOI: 10.1021/jacs.0c02406 • Publication Date (Web): 26 Mar 2020

Record Complexity in the Polycatenation of Three Porous Hydrogen-bonded Organic Frameworks with Stepwise Adsorption Behaviors

Yu-Lin Li, [†] Eugeny V. Alexandrov, [□,//] Qi Yin, [†] Lan Li, [†,‡] Zhi-Bin Fang, [†] Wenbing Yuan, [§,*] Davide M. Proserpio [⊥,□,*] and Tian-Fu Liu [†,‡,*]

[†] State Key Laboratory of Structural Chemistry, Fujian Institute of Research on the Structure of Matter, Chinese Academy of Sciences, Fuzhou 350002, P. R. China.

[□] Samara Center for Theoretical Material Science (SCTMS), Samara State Technical University, Molodogvardeyskaya St. 244, Samara 443100, Russia

[//] Samara Branch of P.N. Lebedev Physical Institute of the Russian Academy of Sciences, Novo-Sadovaya St. 221, Samara 443011, Russia

[‡] University of the Chinese Academy of Sciences, Beijing, 100049, China.

[§] School of Environmental and Chemical Engineering, Foshan University, Foshan, 528000, China.

[⊥] Dipartimento di Chimica, Università degli studi di Milano, Via C. Golgi 19, 20133 Milano, Italy.

KEYWORDS: Hydrogen-bonded Organic Frameworks, Polycatenation, Stepwise Adsorption Behaviors

ABSTRACT: Hydrogen-bonded organic frameworks (HOFs) show great potential in many applications, but few structure-property correlations have been explored in this field. In this work, we report that self-assembly of a rigid and planar ligand gives rise to flat hexagonal honeycomb motifs which are extended into undulated two dimensional (2D) layers and finally generate three polycatenated HOFs with record complexity. This kind of undulation is absent in the 2D layers built from a very similar but non-planar ligand, indicating a slight torsion of ligand produces overwhelming structural change. This change delivers materials with unique stepwise adsorption behaviors under a certain pressure originating from the movement between mutually interwoven hexagonal networks. Meanwhile, high chemical stability, phase transformation, and preferential adsorption of aromatic compounds were observed in these HOFs. The results presented in this work would help us to understand the self-assembly behaviors of HOFs and shed light on the rational design of HOF materials for practical applications.

INTRODUCTION

Learning from the extensively existed hydrogen bonding in the biological system, chemists were inspired to use hydrogen bonding to construct porous frameworks, termed as hydrogen-bonded organic frameworks (HOFs) or supramolecular-organic frameworks (SOFs), as early as 1990s.[1] This kind of materials has many unique advantages including high crystallinity, large surface area, mild synthetic conditions, solvent processability, and so on.[2-6] However, even after the efforts of several decades, the HOFs (including SOFs) field is still under-development especially compared with the prosperousness of its analogue of metal-organic frameworks (MOFs) and covalent organic frameworks (COFs). One of the most significant barriers can be ascribed to the poor chemical stability originated from the weak non-covalent interactions. Apart from stability, another obvious obstacle lies in that the design and prediction of the obtained self-assembly structure is usually unsuccessful, since the rules for self-assembly of HOF have yet to be fully clear.[7-8]

The structures of HOFs were dominated by molecular building blocks that mainly consist of two indispensable parts, namely a backbone (or scaffold) and hydrogen bonding interaction.[9] Changing either of them would make great differences on the obtained structure of materials. For example, self-assembly of the ligand 4,4',4'',4'''-tetra(2,4-diamino-1,3,5-triazin-6-yl)tetra-phenylethene (DAT-TPE) resulted two entirely different HOF structures, where the dissimilarity was derived from the difference on hydrogen bonding interaction.[10-11] Therefore, understanding the influence of both backbone geometry and the hydrogen bonding interaction on the final structure is very important for unveiling the self-assembly rules and realizing the rational design of HOF structures. This encourages us to investigate ligands with identical hydrogen interaction but different backbone geometry. Among these, 4,4',4''-benzene-1,3,5-triyl-tris(benzoic acid) (H_3BTB, also called 1,3,5-tris(4-carboxyphenyl)benzene and abbreviated as TCPB)[12] and 4,4',4''-(1,3,5-tria-zine-2,4,6-triyl)-tribenzoic acid (H_3TATB)[13] (Figure 1)

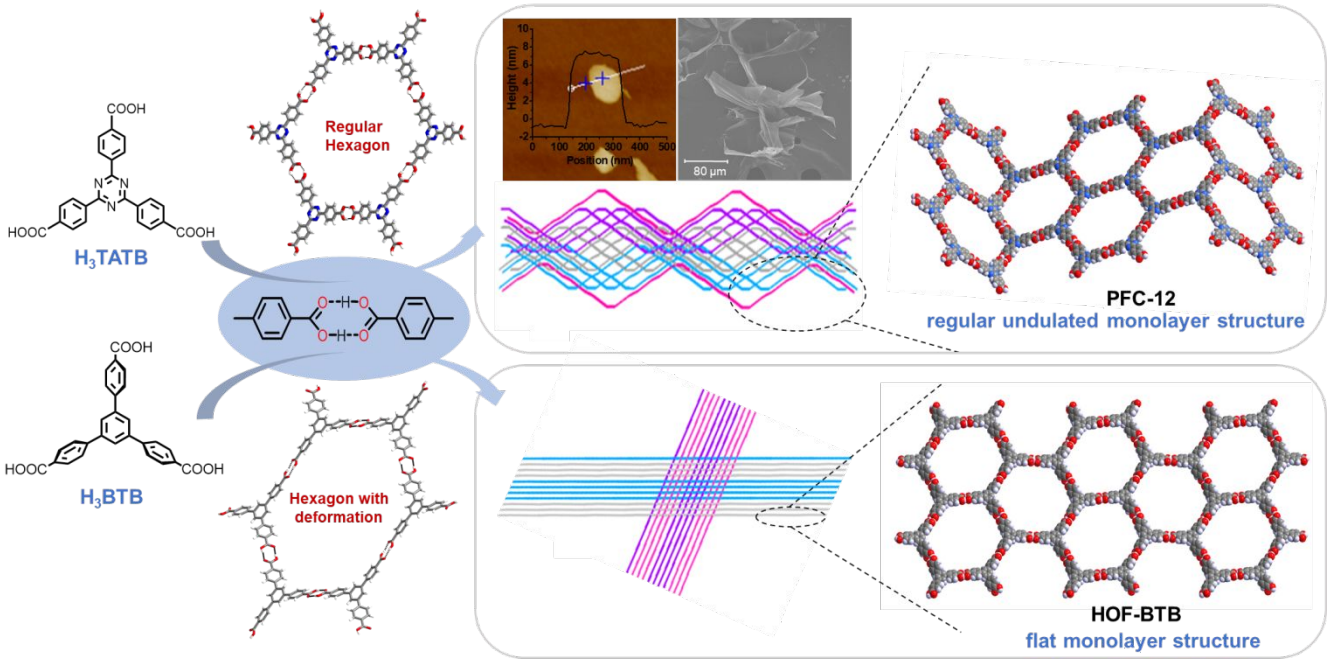

Figure 1. Representation of the chemical structure, the obtained hexagonal honeycomb motifs, the resulted monolayer and polycatenated networks constructed by H_3TATB (upper panel) and H_3BTB (lower panel). Atomic force microscope (AFM) and scanning electron microscope (SEM) images of the solute in supernatant during the crystallization process (fifth and third days, respectively) of **PFC-12** (inset).

attract our interests, because they are readily accessible and the hydrogen interaction between the carboxyl groups on C_3 symmetry backbones can be easily predicted. The difference between these two ligands lies on that H_3TATB is a planar molecule with conjugated effect while H_3BTB is non-planar. The non-planarity of H_3BTB is induced by the slight dihedral angle between adjacent benzene rings.[14] The investigation of the structures assembled from these two ligands would bring us a chance to unveil the factors impacted on the final structure as well as the structure-properties relationship in HOF materials.

In this work, based on the co-planar H_3TATB molecules, three HOFs (**PFC-11**, **PFC-12**, and **PFC-13**) (PFC= Porous materials from FJIRSM, CAS) have been synthesized from different solvents (Scheme S2) and characterized by single-crystal X-ray diffraction. In these structures, adjacent H_3TATB ligands are interconnected through double hydrogen bonds to form regular hexagonal honeycomb nets (**hcb**), which are interwoven simultaneously to form extremely complicated two-dimensional (2D) layer structures. Entanglement (interpenetration or polycatenation) stabilizes structures due to increasing molecular packing density and adding more intermolecular interactions.[15-16] We also speculate that the undulations coupled with parallel polycatenation stabilize the ultra-thin planar fragments formed during self-assembly process, which resembles the microscopic corrugations existing on suspended or supported graphene sheets.[17-20] Undulation of **hcb** nets can be also observed in the HOF structure constructed by other flat molecules of benzene-1,3,5-tricarboxylic acid H_3BTC (named also trimesic acid)[21] and triboronic acid derivative.[22] In contrast, self-assembly of the non-planar H_3BTB molecules (CSD RefCode OGUROZ01) resulted in flat H-bonded **hcb** layers with inclined polycatenation of parallel layers.[14] The entangled structures endow **PFC-11** and **12** with high degree of flexibilities, and therefore expected gate opening adsorption behaviors were observed. The π electrons of s-triazine and phenyl rings on framework provide strong interactions toward molecules with large π conjugation, causing higher uptakes for vapor of benzene and toluene over cyclohexane. The carbon dioxide uptakes are also among highest values for HOFs.[12]

RESULTS AND DISCUSSION

Crystal Structure. **PFC-11**, **12** and **13** were obtained by recrystallization of H_3TATB in ethyl alcohol, isopropanol and the mixture of ethyl alcohol/deionized water, respectively (Scheme S2). Single-crystal X-ray diffraction indicates that H_3TATB monomers in all these structures are interconnected through double hydrogen bonds to form a hexagonal honeycomb motif of **hcb** topology, which is a result of the symmetry of the ligand. Solvent information inside pores was determined by elemental analysis and ^{1}H-NMR (Figure S15-17). Notably, the layers constructed by H_3TATB ligands show regular undulations and these wave-like layers are parallel polycatenated, resulting in intricate crisscrossed 2D networks (Figures 1 and 2). The very high undulation of layers in these structures aroused our attention: the span of the layers in **PFC-11**, **12** and **13** are 49.3 Å, 37.7 Å, and 72.7 Å, respectively. Using ToposPro,[23] we found in CSD only one example of H-bonded organic **hcb** undulated layers that span more than 37 Å: the 1,3,5-triazine-2,4,6-triyltris(4,1-phenylene)triboronic acid with **hcb** topology (OFUVUJ with a span of 53.9 Å).[22] Such high waves have never

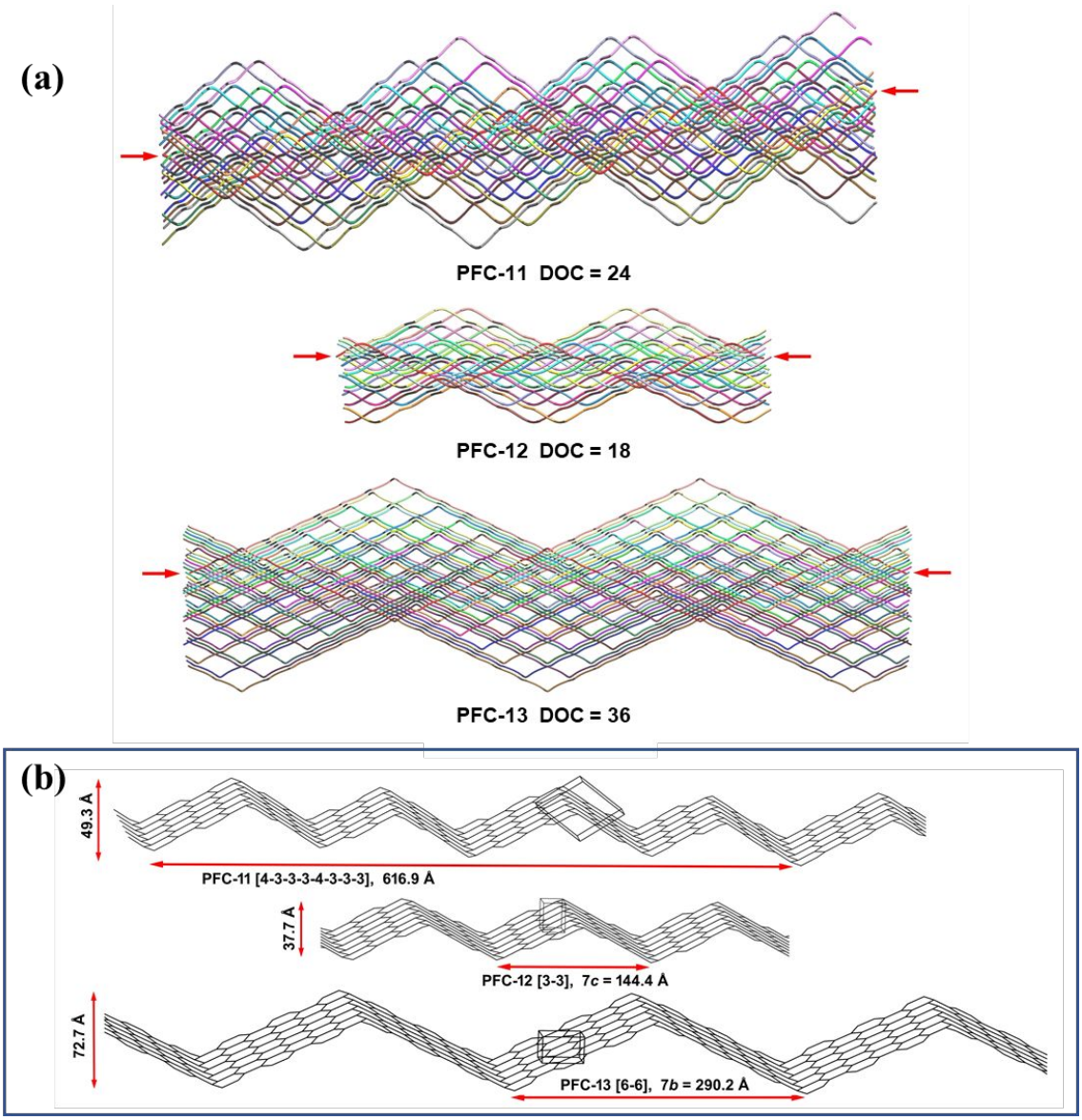

Figure 2. The geometry of entanglement (degree of catenation DOC referred to the red-arrow indicated red layer (a)) and of a single undulated layer (b) for **PFC-11**, **PFC-12**, **PFC-13**.

been observed in other layered H-bonded structures with flat molecular building units.[14, 24-27]

Further looking into the detailed structure of **PFC-11** to **13**, we found that the H_3TATB building units are almost planar molecule (i.e. with deviation from planarity of max. 0.8 Å, see table S2) that self-assembled into a nearly ideally planar hexagonal ring (Figure 1). All the curvature happens on hydrogen interaction sites at interval of specific connection of the hexagons as shown in Figure 2b: 4-3-3-3-4-3-3-3 for **PFC-11** (one step of four hexagons up alternating with three steps of three hexagons down-up-down repeated twice), 3-3 for **PFC-12** (up and down steps of three hexagons), 6-6 for **PFC-13** (six hexagons up and down). Like **PFC-12**, H_3BTC (BTCOAC)[21] has 3-3 steps of hexagon connections but a smaller span of 25.8 vs 37.7 Å due to the smaller size of H_3BTC while the bigger triboronic acid derivative OFUVUJ[22] has 4-4-3-3-4-4-3-3 steps with span 53.9 Å (Table S2).

The origin of the undulation in 2D layered structure. The occurrence of wave-like layers in all these structures, no matter what temperature and solvent we used in the recrystallization process, was reminiscent of the corrugations observed on suspended or supported graphene sheets where the rippling has been invoked to explain the thermodynamic stability of free-standing graphene sheets.[19] There were numerous studies on thin films showing that films become thermodynamically unstable (segregated into islands or decomposed) when the thickness is below a certain value, unless they constitute an inherent part of a three-dimensional (3D) system, such as grown on the surface of a bulk crystal with a matching lattice.[19, 28-29] Therefore, we speculate that during the self-assembly process, the hexagonal motifs constructed by H_3TATB molecules can undergo corrugation after exceeding certain dimension (an undulation step), resulting in undulated layered fragments, or we can say intermediates, which are interwoven simultaneously and finally fixed by molecular packing in a bulk crystal. Moreover, as the hydrogen bond interaction is much labile than the organic

backbones with delocalization of π electrons, the deviation from planarity is manifested in the hydrogen bonding geometry. This speculation is supported by the observation that the supernatant solution contains many lamellae featured about 7 nm in thickness when examined by AFM and SEM analyses, on the fifth and third days during the crystallization process (from different batches, see Figure 1, inset). It is worth to mention that undulated **hcb** were also found in two HOFs built by H_3BTC (BTCOAC)[21] and triboronic acid derivative OFUVUJ[22], which are planar ligands as well. While in a search of H-bonded **hcb** net built from tri-carboxylated ligands, we found that non-planar ligands prefer inclined polycatenation of flat **hcb** nets instead of corrugation (see Table S2). These findings validate our speculation that **hcb** layers distorted by undulation and parallel polycatenation provide higher density of molecular packing and minimize the surface free energy during self-assembly process.

The intricated polycatenation in structures. The parallel polycatenations in **PFC-11**, **PFC-12**, and **PFC-13** have record complexity and unique features, which have never been observed before.[25-27] The three structures are new examples of entanglement isomers with different solvents inside of pores and different topology of rings catenations.[27] In detail, in **PFC-11** one layer (Figure 2a) catenates 24 other layers (degree of catenation, DOC = 24), while rings catenate 12 or 14 other rings (12, 14-c coordination of Hopf ring net, HRN), it is required to remove 20 layers to disjoin the entangled array on two separate parts (index of separation, IS = 20, Figure S1). **PFC-12** has DOC = 18, IS = 14, and 12-c HRN. Finally, **PFC-13** has the record largest DOC = 36 and IS = 35, while 12-c coordination of HRN. The known records on polycatenation complexity of H-bonded networks have been all observed for **hcb** underlying net and are H_3BTC (BTCOAC)[21] with DOC = 10, IS = 8, and 6-c HRN, bis(1,1,1-tris(4-hydroxyphenyl) ethane) tris(4,4'-bipyridyl) (POVJAL)[30] with DOC = 10, IS = 5, and 20-c HRN and the triboronic acid derivative OFUVUJ[22] with DOC = 31, IS = 24, and 14-c HRN. Among coordination polymers, the most complex polycatenation was observed again for **hcb** nets: DOC = 10, IS = 3, 12-c HRN (RIWXIG[31], VUHCUX[32]).

For comparison, we further looked into the structure of HOF-BTB (with the same underlying net **hcb**), where the monolayers are flat and assembled in parallel stacks to form inclined polycatenated 3D array (OGUROZ01).[14] The existence of torsions between adjacent benzene rings of H_3BTB ligands led to the observed hexagonal motif with an obvious deformation out of plane (Figure 1). In this case, we believe that the excess energy was consumed by the rotation of the peripheral phenyl groups (deviation from planarity of max. 1.41 Å), therefore the generated 2D monolayers were flat without undulation. In summary with ToposPro[23], we found in CSD 12 examples of H-bonded networks, with underlying **hcb** nets, from tripodal carboxylate molecules. They show flat networks built from non-planar molecules assembled in inclined polycatenated 3D array (Table S2), again coinciding with our explanation on the origin of the undulated layers in **PFC-11** to **13**. Therefore, a deviation on dihedral angles from planarity produces the overwhelming structural changes observed in this work.

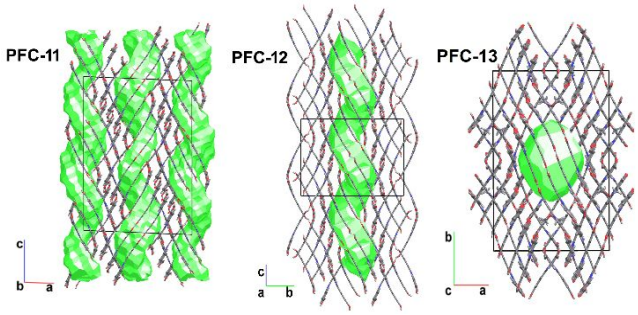

Figure 3. Crystal structures of **PFC-11**, **PFC-12** and **PFC-13** showing the shape of the cavities in green.

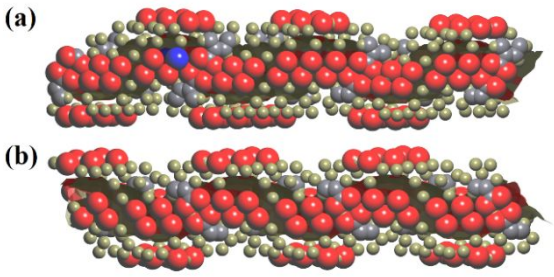

Figure 4. The composition of channel in structures of **PFC-11** (a) and **PFC-12** (b). Balls of olive, red, grey and blue colour present hydrogen, oxygen, carbon, and nitrogen atoms, respectively.

The pore architecture and gas adsorption performance. Despite the presence of intricate polycatenation, there remains solvent-accessible void spaces in **PFC-11**, **PFC-12**, and **PFC-13**, and which are estimated to be 35.2%, 35.2%, and 34.6%, respectively, relative to the whole crystal volumes. Further looking into these structures, **PFC-11** and **PFC-12** obtained from less polar solvents ethyl alcohol and isopropanol exhibit one-dimensional helical open channels, while **PFC-13** obtained from the mixture of ethyl alcohol and H_2O shows closed cavities (Figure 3). Thus, variation of synthesis conditions (choice of solvent) enables tuning the pores geometry and the connections of HOF materials.

The active surface in **PFC-11** and **PFC-12** should exhibit polarity due to the triazine core and carboxylate oxygens in the ligand, as well as sp^2 carbon atoms from aromatic rings peeking out into the pores, that enable stronger interactions with both carbon dioxide and aromatic guest molecules. Thus, the open channels surface in **PFC-11** and **PFC-12** is composed from H, O, C, N in the ratios 60.8:27.4:11.4:0.4 and 64.6:29.2:6.2:0, respectively; **PFC-11** differs from **PFC-12** by presence of N and larger part of sp^2 carbon atoms on the pore surface (Figure 4).

N_2 isotherm shows that **PFC-13** failed to load N_2 after activation, while both **PFC-11** and **PFC-12** exhibit stepwise adsorption isotherms and obvious hysteresis behaviors in the desorption isotherms.[5, 33] As shown in Figure 5a, **PFC-11** and **PFC-12** absorbed N_2 with uptake of 247 cm^3/g and 251 cm^3/g and Brunauer-Emmett-Teller (BET) surface area of 751.3 m^2/g and 653.6 m^2/g, respectively. The well-defined steps occur at low relative pressure ($P/P_0 < 0.09$) and $P/P_0 = 0.36$ during adsorption process. This behavior usually associates with the swelling of non-rigid porous

structures or with irreversible adsorption of molecules in pores of approximately the same size as the adsorbate. Obviously, the radius of nitrogen molecule (1.82-1.90 Å)[34] is much smaller than the pore size of **PFC-11** (the maximal radius of migrating probe Rf = 2.76 Å and radius of maximal pore Rfi = 4.07 Å)[35] and **PFC-12** (Rf = 3.26 Å and Rfi = 3.69 Å) (Figure S4). Therefore, the second step of isotherm at P/P_0 = 0.36 can be ascribed to the movement between mutually interspersed hexagonal networks under a certain pressure. This movement can also explain the unclosed hysteresis loop observed on the desorption branches. In the structure of **PFC-11** and **PFC-12**, the apertures formed by movable polycatenated networks change along with the pressure variation and trap significant amount of adsorbate in pore space during the desorption process. However, this stepwise adsorption behavior was not observed in HOF-BTB as shown in Figure S5 and reference 14 and 36 (two channels along (010) with Rf = 2.76 Å, Rfi = 5.06 Å and Rf = 2.96 Å, Rfi = 4.59 Å), where HOF-BTB displays type I isotherm characteristic of microporosity as most periodic framework materials do. Therefore, it's reasonable to conclude that the wave-like layer structure endows **PFC-11** and **12** with high degree of flexibility and special adsorption behavior.

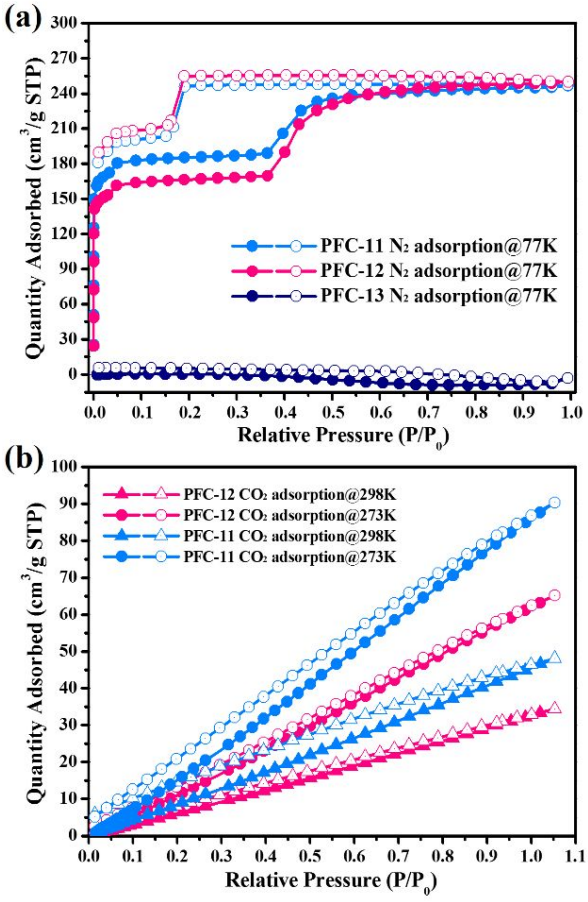

Figure 5. (a) N_2 adsorption isotherms of **PFC-11**, **PFC-12** and **PFC-13** at 77 K. (b) CO_2 adsorption isotherm of **PFC-11** and **PFC-12** at 273 K and 298 K.

The two porous materials were also tested for carbon dioxide adsorption at temperatures 273 K and 298 K (Figure 5b). The resulting isotherms do not show any steps and belong to classical type usually observed in other HOF materials.[4, 8] However, the values of CO_2 uptake in **PFC-11** of 90.3 cm^3/g and 65.1 cm^3/g under pressure 1 atm are among the highest for reported HOFs at 273 K and 298 K, respectively, higher values were obtained before only for HOF-5a.[10, 12] The good CO_2 adsorption capacity can be ascribed to the presence of N and O atoms in the ligands and the H-bonding in framework that polarize the pore surface and make host-guest interactions stronger.

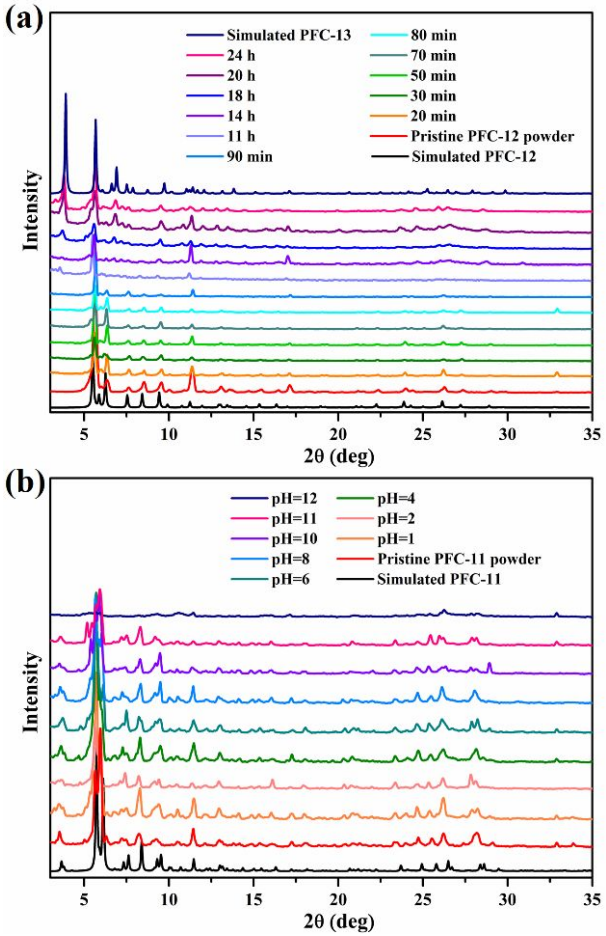

Figure 6. (a) PXRD patterns of **PFC-12, 13** and indicative of the transformation from **PFC-12** to **13** after being soaked in water. (b) PXRD patterns of **PFC-11** after being treated with different pH aqueous solution.

Stability of PFC-11, 12 and 13. Powder X-ray diffraction (PXRD) patterns of **PFC-11**, **PFC-12**, and **PFC-13** after N_2 adsorption are almost identical to those of the pristine samples (Figures S7, S9 and S12), indicating the porous architectures retained after undergoing backbone movement during the adsorption process. Chemical stability test of these compounds demonstrates that both **PFC-11** and **PFC-13** exhibit high water stability in aqueous solution from pH 0 to pH 11 as indicated by PXRD patterns (Figures 6b and S13). Besides, the PXRD patterns of these HOFs still matched well with the simulated patterns after being treated with some organic solvents, such as CH_3OH, acetone, CH_3CN, and CH_2Cl_2 for one day (Figures S8, S10 and S12). Noted that **PFC-12** was transformed to **PFC-13** after being immersed in water for 24 hours as confirmed by PXRD patterns (Figure 6a), indicating a tendency of transformation from a

high porous structure into a close packing phase. As we mentioned above, the variation of synthesis conditions (choice of solvent) enables tuning the pore geometry and their connections. The degree of catenation follows the order of **PFC-12** (DOC = 18) <**PFC-11** (DOC = 24) <**PFC-13** (DOC = 36), which is consistent with the ordered of solvent polarity and molecules dimensions used for recrystallization: isopropanol (for **PFC-12**) < ethanol (for **PFC-11**) < ethanol and water (for **PFC-13**). Therefore, we inferred that the solvent with higher polarity and smaller size produces more closely packed structure. This trend also explains the phenomenon that **PFC-12** can transform to **PFC-13** upon treating with water. Because of the high complexity of the molecular packing, it is difficult to track the structural transformation from **PFC-12** to **PFC-13**. Indeed, the transformation is provided by breaking the H-bonds (the Hopf ring nets are different), as well the closing of pores in the **PFC-12**. Thus, the stacks of 3 molecules of **PFC-12** converts to 6 molecule stacks in **PFC-13** due to the shift of molecules respective to each other (Figure S3).

Vapor adsorption. Inspired by the excellent stability and framework flexibility, the vapor adsorption capacities of **PFC-11** and **PFC-12** toward benzene, toluene, and cyclohexane were investigated. As shown in Figure S18, both **PFC-11** and **PFC-12** have much higher adsorption uptakes of benzene (190.7 cm^3/g for **PFC-11**, 318.7 cm^3/g for **PFC-12**) and toluene (174.9 cm^3/g for **PFC-11**, 183.7 cm^3/g for **PFC-12**) than cyclohexane (91.6 cm^3/g for **PFC-11**, 86.5 cm^3/g for **PFC-12**). The preferential adsorption can be described to the widely exposed π electrons of s-triazine rings in the channel, which can provide strong host-guest interactions toward benzene and toluene molecules.[37-38] The lower adsorption uptake of toluene than benzene can be described to the larger steric hindrance derived from the larger molecular area of toluene (55.3 $Å^2$) than benzene (48.2 $Å^2$).[34] Because of the higher uptake of volatiles for **PFC-12,** we can assume that it undergoes much larger structural changes (the starting pores volume was about the same for both compounds) upon adsorption at pressures more than 0.5 P/P_0. It is also worth noting that both **PFC-11** and **PFC-12** can be recycled through a heating procedure to completely remove the vapor guests (Figures S19), demonstrating **PFC-11** and **PFC-12** are the promising candidates for volatile organic compound adsorption and separation with high stability and uptake.

Conclusion

Based on planar H_3TATB molecules, three HOF materials **PFC-11**, **12**, and **13**, have been synthesized where H_3TATB molecules are connected through double hydrogen bonds to form nearly ideal hexagonal honeycomb motifs. Regular undulations were observed when the hexagonal motifs were extended into a 2D layer, which could be explained by the thermodynamic instability of the layers. Wrinkled layers and entangled networks minimize the free energy and stabilize the entire structure. In contrast, self-assembly of the very similar ligand H_3BTB, bearing the same hydrogen bonding sites but non-planar backbone, resulted in a flat monolayer. The unique interweaving structures of **PFC-11**, **12** and **13** endow materials with high degree of flexibility and stepwise adsorption behavior. With the excellent stability and framework flexibility, **PFC-11** and **12** present promising candidates for carbon dioxide and volatile organic compound adsorption with preferential selectivity toward π-conjugated molecules such as benzene and toluene. This work demonstrated that the slight deviation on dihedral angles in a ligand delivers overwhelmingly changes on both the structure and the property, which allows us to well understand the self-assembly rule and the structure-property relationship for rational design of HOF materials.

ASSOCIATED CONTENT

The Supporting Information is available free of charge via the Internet at http://pubs.acs.org.

Detailed information regarding the experimental methods, syntheses, structure analysis, powder XRD patterns, vapor adsorption (PDF).

Crystallographic data of PFC-11 (CIF)
Crystallographic data of PFC-12 (CIF)
Crystallographic data of PFC-13 (CIF)

AUTHOR INFORMATION

Corresponding Author

* tfliu@fjirsm.ac.cn
* davide.proserpio@unimi.it
* wbyuan@hainanu.edu.cn

Author Contributions

All authors have given approval to the final version of the manuscript.

Notes

The authors declare no competing financial interest.

ACKNOWLEDGMENT

L.T.F. thanks the financial support of National Key Research and Development Program of China (grant No. 2018YFA0208600), "Strategic Priority Research Program" of the Chinese Academy of Sciences (Grant No. XDB20000000). E.V.A. thanks Russian Science Foundation (grant No. 18-73-10116) for financial support of development of methods for topology analysis. D.M.P. thanks the Università degli Studi di Milano for the transition grant PSR2015-1718 and FFABR2018. Y.W. would like to acknowledge the National Natural Science Foundation of China (NSFC, grant no. 21561009) for financial support.

ABBREVIATIONS

PFC = Porous materials from FJIRSM, CAS;
CAS = Chinese Academy of Sciences
DOC = degree of catenation
IS = index of separation

REFERENCES

(1) Hisaki, I.; Nakagawa, S.; Ikenaka, N.; Imamura, Y.; Katouda, M.; Tashiro, M.; Tsuchida, H.; Ogoshi, T.; Sato, H.; Tohnai, N.; Miyata, M., A Series of Layered Assemblies of Hydrogen-Bonded, Hexagonal Networks of C3-Symmetric pi-Conjugated Molecules: A Potential Motif of Porous Organic Materials. *J Am Chem Soc* **2016,** *138* (20), 6617-6628.

(2) Hu, F.; Liu, C.; Wu, M.; Pang, J.; Jiang, F.; Yuan, D.; Hong, M., An Ultrastable and Easily Regenerated Hydrogen-Bonded Organic Molecular Framework with Permanent Porosity. *Angew Chem Int Ed* **2017,** *56* (8), 2101-2104.

(3) Yin, Q.; Zhao, P.; Sa, R. J.; Chen, G. C.; Lu, J.; Liu, T. F.; Cao, R., An Ultra-Robust and Crystalline Redeemable Hydrogen-Bonded Organic Framework for Synergistic Chemo-Photodynamic Therapy. *Angew Chem Int Ed* **2018,** *57* (26), 7691-7696.

(4) Lu, J.; Cao, R., Porous Organic Molecular Frameworks with Extrinsic

Porosity: A Platform for Carbon Storage and Separation. *Angew Chem Int Ed* **2016,** *55* (33), 9474-9480.

(5) Yin, Q.; Li, Y. L.; Li, L.; Lu, J.; Liu, T. F.; Cao, R., Novel Hierarchical Meso-Microporous Hydrogen-Bonded Organic Framework for Selective Separation of Acetylene and Ethylene versus Methane. *ACS Appl Mater Interfaces* **2019,** *11* (19), 17823-17827.

(6) Patil, R. S.; Banerjee, D.; Zhang, C.; Thallapally, P. K.; Atwood, J. L., Selective CO_2Adsorption in a Supramolecular Organic Framework. *Angew Chem Int Ed* **2016,** *128* (14), 4599-4602.

(7) Hisaki, I.; Xin, C.; Takahashi, K.; Nakamura, T., Designing Hydrogen-Bonded Organic Frameworks (HOFs) with Permanent Porosity. *Angew Chem Int Ed* **2019**,58(33), 11160-11170.

(8) Lin, R. B.; He, Y.; Li, P.; Wang, H.; Zhou, W.; Chen, B., Multifunctional porous hydrogen-bonded organic framework materials. *Chem Soc Rev* **2019,** *48* (5), 1362-1389.

(9) Han, Y. F.; Yuan, Y. X.; Wang, H. B., Porous Hydrogen-Bonded Organic Frameworks. *Molecules* **2017,** *22* (2), 266.

(10) Wang, H.; Li, B.; Wu, H.; Hu, T. L.; Yao, Z.; Zhou, W.; Xiang, S.; Chen, B., A Flexible Microporous Hydrogen-Bonded Organic Framework for Gas Sorption and Separation. *J Am Chem Soc* **2015,** *137* (31), 9963-9970.

(11) Wang, H.; Bao, Z.; Wu, H.; Lin, R. B.; Zhou, W.; Hu, T. L.; Li, B.; Zhao, J. C.; Chen, B., Two solvent-induced porous hydrogen-bonded organic frameworks: solvent effects on structures and functionalities. *Chem Commun* **2017,** *53* (81), 11150-11153.

(12) Yang, W.; Zhou, W.; Chen, B., A Flexible Microporous Hydrogen-Bonded Organic Framework. *Crystal Growth & Design* **2019,** *19* (9), 5184-5188.

(13) Muhlbauer, E.; Klinkebiel, A.; Beyer, O.; Auras, F.; Wuttke, S.; Luning, U.; Bein, T., Functionalized PCN-6 metal-organic frameworks. *Microporous and Mesoporous Materials* **2015,** *216*, 51-55.

(14) Zentner, C. A.; Lai, H. W.; Greenfield, J. T.; Wiscons, R. A.; Zeller, M.; Campana, C. F.; Talu, O.; FitzGerald, S. A.; Rowsell, J. L., High surface area and Z' in a thermally stable 8-fold polycatenated hydrogen-bonded framework. *Chem Commun* **2015,** *51* (58), 11642-11645.

(15) Baburin, I. A.; Leoni, S., Modelling polymorphs of metal–organic frameworks: a systematic study of diamondoid zinc imidazolates. *CrystEngComm* **2010,** *12* (10), 2809-2816.

(16) Alexandrov, E. V.; Blatov, V. A.; Proserpio, D. M., Interpenetration of three-periodic networks in crystal structures: Description and classification methods, geometrical-topological conditions of implementation. *Journal of Structural Chemistry* **2015,** *55* (7), 1308-1325.

(17) Stöberl, U.; Wurstbauer, U.; Wegscheider, W.; Weiss, D.; Eroms, J., Morphology and flexibility of graphene and few-layer graphene on various substrates. *Applied Physics Letters* **2008,** *93* (5), 051906.

(18) Meyer, J. C.; Geim, A. K.; Katsnelson, M. I.; Novoselov, K. S.; Booth, T. J.; Roth, S., The structure of suspended graphene sheets. *Nature* **2007,** *446* (7131), 60-63.

(19) Lui, C. H.; Liu, L.; Mak, K. F.; Flynn, G. W.; Heinz, T. F., Ultraflat graphene. *Nature* **2009,** *462* (7271), 339-341.

(20) Fasolino, A.; Los, J. H.; Katsnelson, M. I., Intrinsic ripples in graphene. *Nat Mater* **2007,** *6* (11), 858-861.

(21) Duchampt, D. J.; Marsh, R. E., The Crystal Structure of Trimesic Acid (Benzene-l, 3, 5-triearboxylic Acid). *Acta Cryst* **1969,** *B25*, 5-19.

(22) Sarkar, K.; Dastidar, P., Supramolecular Hydrogel Derived from a C3-Symmetric Boronic Acid Derivative for Stimuli-Responsive Release of Insulin and Doxorubicin. *Langmuir* **2018,** *34* (2), 685-692.

(23) Blatov, V. A.; Shevchenko, A. P.; Proserpio, D. M., Applied Topological Analysis of Crystal Structures with the Program Package ToposPro. *Crystal Growth & Design* **2014,** *14* (7), 3576-3586.

(24) Chen, T. H.; Popov, I.; Kaveevivitchai, W.; Chuang, Y. C.; Chen, Y. S.; Daugulis, O.; Jacobson, A. J.; Miljanic, O. S., Thermally robust and porous noncovalent organic framework with high affinity for fluorocarbons and CFCs. *Nat Commun* **2014,** *5*, 5131.

(25) Zolotarev, P. N.; Arshad, M. N.; Asiri, A. M.; Al-amshany, Z. M.; Blatov, V. A., A Possible Route toward Expert Systems in Supramolecular Chemistry: 2-Periodic H-Bond Patterns in Molecular Crystals. *Crystal Growth & Design* **2014,** *14* (4), 1938-1949.

(26) Carlucci, L.; Ciani, G.; Proserpio, D. M.; Mitina, T. G.; Blatov, V. A., Entangled two-dimensional coordination networks: a general survey. *Chem Rev* **2014,** *114* (15), 7557-7580.

(27) Alexandrov, E. V.; Blatov, V. A.; Proserpio, D. M., How 2-periodic coordination networks are interweaved: entanglement isomerism and polymorphism. *Crystengcomm* **2017,** *19* (15), 1993-2006.

(28) Zinke-Allmang, M.; Feldman, L. C.; Grabow, M. H., Clustering on surfaces. *Surface Science Reports* **1992,** *16* (8), 377-463.

(29) Evans, J. W.; Thiel, P. A.; Bartelt, M. C., Morphological evolution during epitaxial thin film growth: Formation of 2D islands and 3D mounds. *Surface Science Reports* **2006,** *61* (1-2), 1-128.

(30) Bényei, A. C.; Coupar, P. I.; Ferguson, G.; Glidewell, C.; Lough, A. J.; Meehan, P. R., Tenfold Interpenetration of Giant HexagonalR1212(126) Nets in the Hydrogen-Bonded Structure of 1,1,1-Tris(4-hydroxyphenyl)ethane–4,4'-Bipyridyl (2/3). *Acta Cryst* **1998,** *E54* (10), 1515-1519.

(31) Jiang, X.; Li, Z.; Zhai, Y.; Yan, G.; Xia, H.; Li, Z., Porous coordination polymers based on azamacrocyclic complex: syntheses, solvent-induced reversible crystal-to-crystal transformation and gas sorption properties. *CrystEngComm* **2014,** *16* (5), 805-813.

(32) Yang, Q. Y.; Zheng, S. R.; Yang, R.; Pan, M.; Cao, R.; Su, C. Y., An unusual 3D coordination polymer assembled through parallel interpenetrating and polycatenating of (6,3) nets. *CrystEngComm* **2009,** *11* (4), 680-685.

(33) Burtch, N. C.; Jasuja, H.; Walton, K. S., Water stability and adsorption in metal-organic frameworks. *Chem Rev* **2014,** *114* (20), 10575-10612.

(34) Li, J. R.; Kuppler, R. J.; Zhou, H. C., Selective gas adsorption and separation in metal-organic frameworks. *Chem Soc Rev* **2009,** *38* (5), 1477-1504.

(35) Blatova, O. A.; Golov, A. A.; Blatov, V. A., Natural tilings and free space in zeolites: models, statistics, correlations, prediction. *Z Krist-Cryst Mater* **2019,** *234* (7-8), 421-436.

(36) Yoon, T. U.; Baek, S. B.; Kim, D.; Kim, E. J.; Lee, W. G.; Singh, B. K.; Lah, M. S.; Bae, Y. S.; Kim, K. S., Efficient separation of C2 hydrocarbons in a permanently porous hydrogen-bonded organic framework. *Chem Commun* **2018,** *54* (67), 9360-9363.

(37) Huang, Y.; Lin, Z.; Fu, H.; Wang, F.; Shen, M.; Wang, X.; Cao, R., Porous anionic indium-organic framework with enhanced gas and vapor adsorption and separation ability. *ChemSusChem* **2014,** *7* (9), 2647-2653.

(38) Liu, T. F.; Lu, J.; Lin, X.; Cao, R., Construction of a trigonal bipyramidal cage-based metal-organic framework with hydrophilic pore surface via flexible tetrapodal ligands. *Chem Commun* **2010,** *46* (44), 8439-8441.

Table of Contents (TOC)/Abstract Graphic

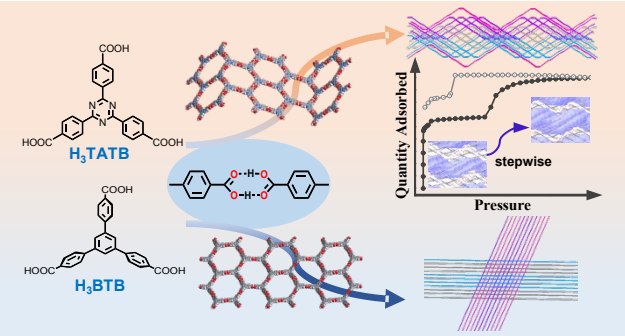
COOH
HOOC
COOH
H3TATB
COOH
HOOC
COOH
H3BTB
Quantity Adsorbed
Pressure
stepwise